

# An effective route to improve the catalytic performance of SAPO-34 in the methanol-to-olefin reaction

Guangyu Liu<sup>1,2</sup>, Peng Tian<sup>1</sup>, Qinhua Xia<sup>3</sup>, Zhongmin Liu<sup>1\*</sup>

1. National Engineering Laboratory for Methanol to Olefin, Dalian Institute of Chemical Physics, Chinese Academy of Sciences, Dalian 116023, Liaoning, China; 2. School of Chemistry and Chemical Engineering, Henan University of Technology, Zhengzhou 450001, Henan, China; 3. Ministry of Education Key Laboratory for the Synthesis and Application of Organic Functional Molecules, School of Chemistry and Chemical Engineering, Hubei University, Wuhan 430062, Hubei, China

[Manuscript received January 11, 2012; revised April 6, 2012]

## Abstract

An effective route to improve the catalytic performance of SAPO-34 in the methanol-to-olefin reaction by simple oxalic acid treatment was investigated. The samples were characterized by XRD, SEM, N<sub>2</sub> adsorption-desorption, XRF, TG, <sup>29</sup>Si MAS NMR and NH<sub>3</sub>-TPD techniques. The results indicated that the external surface acidity of SAPO-34 was finely tuned by oxalic acid treatment, and the selectivity to C<sub>2</sub>H<sub>4</sub> on SAPO-34 and the catalyst lifetime in the methanol-to-olefin reaction were greatly improved.

## Key words

SAPO-34; methanol-to-olefin (MTO); oxalic acid; modification; acidity

## 1. Introduction

Methanol-to-olefin (MTO) reaction has been attracting much attention because it is the key step as a non-oil route to produce ethylene and propylene. SAPO-34 is currently recognized as the desired catalyst for the MTO reaction, due to its small pore, moderate acidity and excellent thermal/hydrothermal stability [1,2]. Up to now, researches on the MTO reaction are mainly focused on the reaction mechanism and the effect of different synthesis parameters of SAPO-34 on the reaction [3–11]. Few studies put emphasis upon the post-synthesis modification of SAPO-34 to improve its catalytic performance in the MTO reaction [12–16].

It has been recognized that the Si amount in SAPO-34 is the unique factor for controlling the catalyst acidity, relatively important for improving the catalyst lifetime and the selectivity of light olefins in the MTO reaction, for which SAPO-34 with a low Si content is required [17,18]. However, our previous results showed that the crystallization yield of SAPO-34 dropped with decreasing Si content in the synthesis gel, especially in the range of low Si content. And, the Si distribution in crystals was not homogeneous, showing a gradual increase from the core to the shell; i.e., the Si environment was only Si(4Al) in the initially formed core and other Si environments

would appear with the growth of crystal size during the crystallization [19]. This implies the unnecessary to crystallize a special SAPO-34 catalyst with low Si content in order to obtain good MTO results. In the present paper, we report a simple and effective post-synthesis method to corrode the external surface of SAPO-34 crystals with ‘higher’ Si content by oxalic acid solution, and to tune the surface acidity further. Interestingly, very encouraging improvement of catalytic performance has been achieved.

## 2. Experimental

### 2.1. Catalyst preparation

SAPO-34 was hydrothermally synthesized from the gel with a molar composition of 1.5 diethylamine (DEA) : 1.0 Al<sub>2</sub>O<sub>3</sub> : 0.8 P<sub>2</sub>O<sub>5</sub> : 0.4 SiO<sub>2</sub> : 50 H<sub>2</sub>O. The detailed synthesis procedure has been described elsewhere [20]. Post-synthesis treatment of as-synthesized SAPO-34 was carried out at room temperature for 6 h with a solution of oxalic acid (solution/solid = 2 mL/g). The catalysts were obtained by calcining the modified samples at 550 °C in air for 5 h and designated as SAPO-*x*M (*x* is the concentration of oxalic acid solution).

\* Corresponding author. Tel/Fax: +86-411-84685510; E-mail: [liuzm@dicp.ac.cn](mailto:liuzm@dicp.ac.cn)

## 2.2. Catalytic activity measurements

MTO reaction was carried out with a fixed-bed reactor at atmospheric pressure. 1.5 g of catalyst (20~40 mesh) was loaded into the reactor. The sample was pretreated in a flow of dry nitrogen at 550 °C for 1 h and then the temperature of reactor was reduced to 450 °C. The mixture (the weight ratio of CH<sub>3</sub>OH/H<sub>2</sub>O was 40/60) was pumped into the reactor after nitrogen was turned off. The weight hourly space velocity (WHSV) was 2 h<sup>-1</sup>. The products were analyzed on-line by a Varian GC3800 gas chromatograph equipped with a FID detector and a PoraplotQ-HT capillary column.

## 2.3. Characterization

The powder XRD pattern was recorded on a Rigaku D/MAX-γB X-ray diffractometer with Cu K<sub>α</sub> radiation (λ = 0.15406 nm). The chemical composition of the sample was determined with a Philips Magix-601 X-Ray Fluorescence (XRF) spectrometer. The crystal morphology was analyzed by scanning electron microscopy (SEM, KYKY-AMRAY-1000B). <sup>29</sup>Si MAS NMR spectroscopy measurement was conducted at resonance frequencies of 79.41 MHz, using a Varian Infinity plus 400 WB spectrometer. The spinning rates of the samples at the magic angle were 4 kHz. The reference material for the chemical shift (in ppm) was 2, 2-dimethyl-2-silapentane-5-sulfonate sodium salt (DSS). The thermal analysis was performed on a TA Q600 analyzer

with the temperature-programmed rate of 10 °C/min under air flow. The textural data were obtained by nitrogen adsorption measurement using a Micromeritics 2010 analyzer. Before analysis all samples were degassed at 350 °C under vacuum. The temperature-programmed desorption of ammonia (NH<sub>3</sub>-TPD) was carried out with an Autochem 2910 equipment (Micromeritics). Ammonia was injected in order to saturate the sample surface at 100 °C. Prior to the injection, the sample (200 mg) was activated at 650 °C for 40 min (10 °C/min) under He (20 cm<sup>3</sup>/min). The measurement of the desorbed NH<sub>3</sub> was performed from 100 °C to 650 °C (10 °C/min) under He (40 cm<sup>3</sup>/min).

## 3. Results and discussion

The MTO reaction results on catalysts are listed in Table 1. Very clearly, the selectivity of C<sub>2</sub>H<sub>4</sub> was notably increased over post-modified samples. Moreover, both the total selectivity of (C<sub>2</sub>H<sub>4</sub>+C<sub>3</sub>H<sub>6</sub>) and the ratio of C<sub>2</sub>H<sub>4</sub>/C<sub>3</sub>H<sub>6</sub> were higher over modified samples than those on the parent SAPO-34. The best catalytic activity and selectivity were realized over the sample SAPO-0.2M modified by 0.2 M oxalic acid solution. For example, the selectivity of C<sub>2</sub>H<sub>4</sub> was increased from 41.6% to 45.7%, and the on-stream lifetime of catalyst was extended from 82 min to 130 min. However, a further increase of oxalic acid concentration led to an appreciable drop of the on-stream lifetime of the treated sample to 66 min.

Table 1. MTO results on samples modified by oxalic acid

Sample	TOS (min)	Selectivity (wt%)								
		CH <sub>4</sub>	C <sub>2</sub> H <sub>4</sub>	C <sub>2</sub> H <sub>6</sub>	C <sub>3</sub> H <sub>6</sub>	C <sub>3</sub> H <sub>8</sub>	C <sub>4</sub>	C <sub>5+</sub>	C <sub>2</sub> <sup>=</sup> /C <sub>3</sub> <sup>=</sup>	C <sub>2</sub> <sup>=</sup> +C <sub>3</sub> <sup>=</sup>
SAPO-34	2	0.8	33.2	0.4	40.7	4.4	16.9	3.6	0.81	73.8
	82*	1.2	41.6	0.7	39.6	2.1	12.1	2.7	1.05	81.2
SAPO-0.1M	2	0.8	34.6	0.5	41.1	4.9	15	3	0.84	75.7
	82*	1.4	44.3	0.8	38.4	2.4	10.6	2.2	1.15	82.6
SAPO-0.2M	2	0.8	34.5	0.5	40.6	4.8	15.8	3.1	0.85	75
	130*	1.7	45.7	0.8	37.9	1.8	10.1	2.2	1.21	83.6
SAPO-0.4M	2	1.5	35.1	0.6	40.5	4.3	14.8	3.2	0.87	75.6
	66*	1.4	44.6	0.7	38.4	2	10.6	2.3	1.16	83

Reaction conditions: WHSV = 2 h<sup>-1</sup>, T = 450 °C, 40 wt% methanol-water solution; \* Lifetime: the reaction duration with >99% methanol conversion

XRD results given in Table 2 show that the relative crystallinity of the samples decreased with increasing oxalic acid concentration and SAPO-0.4M had the lowest value of 74%.

Figure 1 presents the SEM images of SAPO-34 and modified samples. The crystal surfaces of the modified samples have become rough, especially for the sample SAPO-0.4M.

Table 2. Relative crystallinity and chemical composition of samples

Sample	Relative crystallinity (%)	Mole composition
SAPO-34	100	Al <sub>0.493</sub> P <sub>0.421</sub> Si <sub>0.086</sub>
SAPO-0.1M	95	Al <sub>0.495</sub> P <sub>0.423</sub> Si <sub>0.082</sub>
SAPO-0.2M	82	Al <sub>0.495</sub> P <sub>0.425</sub> Si <sub>0.080</sub>
SAPO-0.4M	74	Al <sub>0.497</sub> P <sub>0.429</sub> Si <sub>0.074</sub>

Figure 2 illustrates the N<sub>2</sub> adsorption-desorption isotherms of different samples at 77 K. The N<sub>2</sub> adsorption-desorption isotherms of SAPO-34 and SAPO-0.1M are of type I with a plateau at higher relative pressures and no distinct hysteresis loop, which is typical for a microporous material without significant mesoporosity. Although the isotherm of SAPO-0.4M is also of type I, it has a hysteresis loop between p/p<sub>0</sub> = 0.5~0.95, which means the appearance of mesoporous structure. The textural properties of different samples are presented in Table 3. The micropore volume and surface area of samples dropped gradually after modification treatment, but accompanied by the appearance of mesopore volume and external surface area.

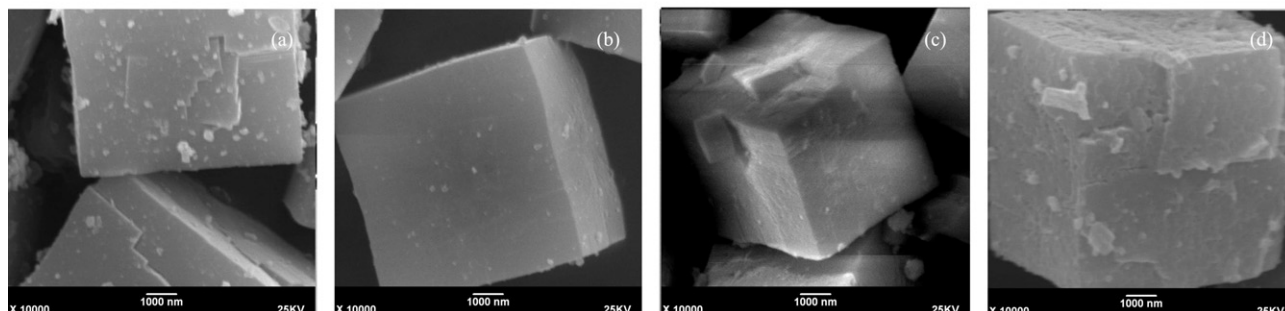


Figure 1. SEM images of (a) SAPO-34 (b) SAPO-0.1M (c) SAPO-0.2M and (d) SAPO-0.4M

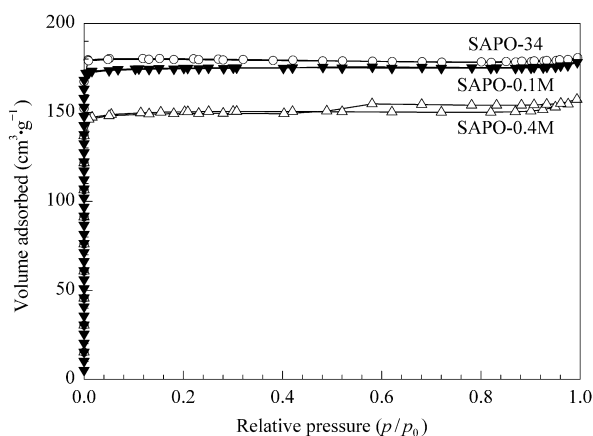


Figure 2. N<sub>2</sub> adsorption-desorption isotherms of samples

Table 3. Textural properties of samples

Sample	Surface area (m <sup>2</sup> /g)			Pore volume (cm <sup>3</sup> /g)		
	$S_{\text{micro}}$	$S_{\text{external}}$	$S_{\text{total}}$	$V_{\text{micro}}$	$V_{\text{meso}}$	$V_{\text{total}}$
SAPO-34	559	0	559	0.28	0	0.28
SAPO-0.1M	538	9	547	0.27	0	0.27
SAPO-0.4M	463	13	476	0.23	0.02	0.25

Table 4 presents the thermal analysis results of samples. The template amount occluded inside the framework was close to that of SAPO-34, implying the untouched interior of the crystals. Therefore, it is concluded from the above information that the damage to the crystalline SAPO-*x*M samples during oxalic acid treatment only occurred on the external surface of the crystals.

Table 4. Thermal analysis results of samples

Sample	H <sub>2</sub> O weight loss (%) I (<185 °C)	Template weight loss (%)		
		II (185–450 °C)	III (>450 °C)	II+III
SAPO-34	2.66	8.08	4.59	12.67
SAPO-0.2M	2.52	8.94	3.72	12.66
SAPO-0.4M	3.73	9.34	3.37	12.71

<sup>29</sup>Si MAS NMR was performed to investigate the Si environment in the samples. As one can see from Figure 3, different Si environments co-exist in the framework of SAPO-34 and modified samples. The deconvoluted results in Table 5 show that the percentage of Si(4Al) in the treated

samples gradually rose following up the increase of oxalic acid concentration until only Si(4Al) environment emerged in SAPO-0.4M. This means that the occurrence of desalination phenomenon during the post treatment mainly removed Si atoms from Si-rich areas, which is contradictory to one common sense that oxalic acid is usually used as a dealumination reagent. Considering rough external surface of the treated samples and previous finding of ‘Si enrichment on the SAPO-34 surface’ [19], we can come to a conclusion that oxalic acid treatment caused an entire corrosion of external crystal surface, not merely occurring on the Si sites.

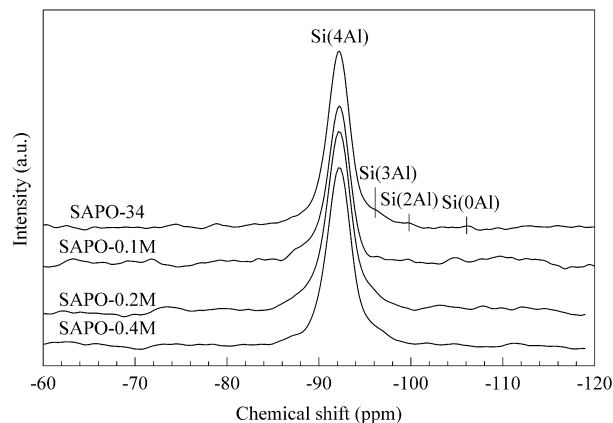


Figure 3. <sup>29</sup>Si MAS NMR spectra of different samples

Table 5. Distribution of Si environments obtained from deconvoluted <sup>29</sup>Si MAS NMR spectra

Sample	Silicon environment distribution (%)			
	Si(4Al)	Si(3Al)	Si(2Al)	Si(0Al)
SAPO-34	86.0	10.0	2.3	1.7
SAPO-0.1M	90.8	9.2	0	0
SAPO-0.2M	92.2	7.8	0	0
SAPO-0.4M	100	0	0	0

Elemental analysis was used to detect the change of the sample compositions, and the results are presented in Table 2. Si content in the samples decreased obviously with the severity of the post treatment, but both the alumina and phosphate contents increased a little, which is in agreement with the results of SEM and <sup>29</sup>Si MAS NMR.

It seems that the variation in the catalytic performance may be related to the change of Si environment in the modified samples. After oxalic acid treatment, the Si environment in the crystals became more uniform and the acidity on the external surface of crystals decreased due to the removal of Si from Si islands. Results from  $\text{NH}_3$ -TPD given in Figure 4 and Table 6 confirmed that both the acid strength and the acid number of the samples decreased following oxalic acid treatment. The percentage of the strong acid sites in the total acid number decreased from 27% in SAPO-34 to 20% in SAPO-0.4M.

According to the present results, the external acidity of SAPO-34 crystal had important influence on the MTO reaction. The acidity arising from Si island would lead to the decrease of catalyst lifetime and the drop of the selectivity of  $\text{C}_2\text{H}_4$ , which was due to the higher acid strength and the acid density. The change of MTO reaction in the present work was also consistent with our previous investigation—SAPO-34 synthesized hydrothermally with higher Si content in the framework shortened the catalyst lifetime and decreased the  $\text{C}_2\text{H}_4$  selectivity [20]. Mores et al. [21] once reported that large carbonaceous deposits formed in the cages at the edge of the SAPO-34 crystal prevented the reaction front to move to-

wards the centre of the crystal leading to fast catalyst deactivation, suggesting that the acid sites close to the external surface played an important role in the reaction, in agreement well with the present work. The drop in the lifetime of SAPO-0.4M may be ascribed to its low crystallinity and surface area.

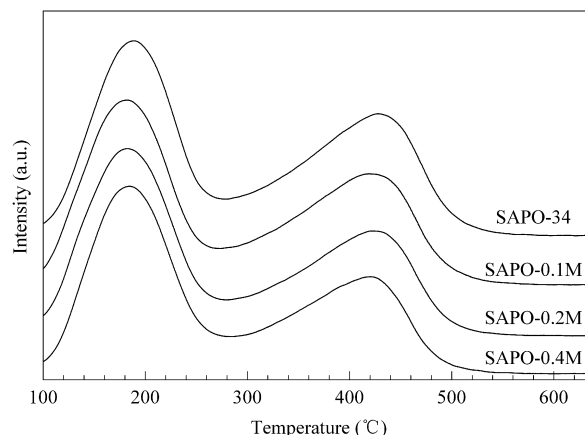


Figure 4.  $\text{NH}_3$ -TPD profiles of different samples

Table 6. Acidity of samples from  $\text{NH}_3$ -TPD

Sample	Weak acidity		Medium acidity		Strong acidity		Total (%)
	T (°C)	percentage (%)	T (°C)	percentage (%)	T (°C)	percentage (%)	
SAPO-34	187	51	351	22	429	27	100.0
SAPO-0.1M	181	51	343	20	421	26	97
SAPO-0.2M	181	51	342	18	422	24	93
SAPO-0.4M	184	50	343	19	421	20	89

#### 4. Conclusions

SAPO-34 was modified by oxalic acid solution. The results indicate that the external surface of SAPO-34 crystals is corroded and the relative crystallinity decreases after the modification treatment. The micropore volume and surface area of SAPO-34 drops after modification, but accompanies by the appearance of mesopore volume and external surface area. The modified samples exhibit higher selectivity of  $\text{C}_2\text{H}_4$  and longer catalyst lifetime in MTO reaction than the parent SAPO-34. The phenomena can be assigned to the decrease of acidity strength and acid site density on the external surface of SAPO-34 crystals induced by removing Si atoms from Si-rich areas. In summary, our results presented here indicate that the post-treatment modification is an effective tool on enhancing the catalytic MTO performance of SAPO-34.

#### References

- [1] Liang J, Li H Y, Zhao S Q, Guo W G, Wang R H, Ying M L. *Appl Catal*, 1990, 64(1): 31
- [2] Stöcker M. *Microporous Mesoporous Mater*, 1999, 29(1-2): 3
- [3] Song W G, Fu H, Haw J F. *J Am Chem Soc*, 2001, 123(20): 4749
- [4] Hunger M, Seiler M, Buchholz A. *Catal Lett*, 2001, 74(1-2): 61
- [5] Jiang Y J, Wang W, Marthala V R R, Huang J, Sulikowski B, Hunger M. *J Catal*, 2006, 238(1): 21
- [6] Arstad B, Kolboe S. *J Am Chem Soc*, 2001, 123(33): 8137
- [7] Cui Z M, Liu Q, Song W G, Wan L J. *Angew Chem Int Ed*, 2006, 45(39): 6512
- [8] Wang Y D, Wang C M, Liu H X, Xie Z K. *Chin J Catal (Cuihua Xuebao)*, 2010, 31(1): 33
- [9] Li P, Zhang W P, Han X W, Bao X H. *Chin J Catal (Cuihua Xuebao)*, 2011, 32(2): 293
- [10] Zhang J C, Zhang H B, Yang X Y, Huang Z, Cao W L. *J Nat Gas Chem*, 2011, 20(3): 266
- [11] Liu G Y, Tian P, Liu Z M. *Chin J Catal (Cuihua Xuebao)*, 2012, 33(1): 174
- [12] Song W G, Haw J F. *Angew Chem Int Ed*, 2003, 42(8): 892
- [13] Mees F D P, Van Der Voort P, Cool P, Martens L R M, Janssen M J G, Verberckmoes A A, Kennedy G J, Hall R B, Wang K, Vansant E F. *J Phys Chem B*, 2003, 107(14): 3161
- [14] Inui T, Kang M. *Appl Catal A*, 1997, 164(1-2): 211
- [15] Kang M. *J Mol Catal A*, 2000, 160(2): 437
- [16] Zhu Z D, Hartmann M, Kevan L. *Chem Mater*, 2000, 12(9): 2781
- [17] Wilson S, Barger P. *Microporous Mesoporous Mater*, 1999, 29(1-2): 117
- [18] Izadbakhsh A, Farhadi F, Khorasheh F, Sahebdeifar S, Asadi M, Yan Z F. *Microporous Mesoporous Mater*, 2009, 126(1-2): 1
- [19] Liu G Y, Tian P, Zhang Y, Li J Z, Xu L, Meng S H, Liu Z M. *Microporous Mesoporous Mater*, 2008, 114(1-3): 416
- [20] Liu G Y, Tian P, Li J Z, Zhang D Z, Zhou F, Liu Z M. *Microporous Mesoporous Mater*, 2008, 111(1-3): 143
- [21] Mores D, Stavitski E, Kox M H F, Kornatowski J, Olsbye U, Weckhuysen B M. *Chem Eur J*, 2008, 14(36): 11320